

## Treatment of modelling uncertainty of NLFEA in fib Model Code 2020

Engen, Morten; Hendriks, Max A.N.; Monti, Giorgio; Allaix, Diego L.

**DOI**

[10.1002/suco.202100420](https://doi.org/10.1002/suco.202100420)

**Publication date**

2021

**Document Version**

Final published version

**Published in**

Structural Concrete

**Citation (APA)**

Engen, M., Hendriks, M. A. N., Monti, G., & Allaix, D. L. (2021). Treatment of modelling uncertainty of NLFEA in fib Model Code 2020. *Structural Concrete*, 22(6), 3202-3212.  
<https://doi.org/10.1002/suco.202100420>

**Important note**

To cite this publication, please use the final published version (if applicable).  
Please check the document version above.

**Copyright**

Other than for strictly personal use, it is not permitted to download, forward or distribute the text or part of it, without the consent of the author(s) and/or copyright holder(s), unless the work is under an open content license such as Creative Commons.

**Takedown policy**

Please contact us and provide details if you believe this document breaches copyrights.  
We will remove access to the work immediately and investigate your claim.



## DESIGN TO BUILD COMPETENCE IN PRECAST


### THE BEST SOLUTIONS FOR YOUR PRECAST PROJECTS

- > Automated workflows to accelerate design and detailing processes
- > Automated creation of shop drawings and production data
- > Quality assured data for ERP and MES

FIND OUT MORE NOW:  
[allplan-precaster.com](http://allplan-precaster.com)

## ARTICLE

# Treatment of modelling uncertainty of NLFEA in *fib* Model Code 2020

Morten Engen<sup>1,2</sup>  | Max A. N. Hendriks<sup>2,3</sup> | Giorgio Monti<sup>4,5</sup> | Diego L. Allaix<sup>6,7</sup>

<sup>1</sup>Multiconsult Norge AS, Oslo, Norway

<sup>2</sup>Department of Structural Engineering, NTNU, Norwegian University of Science and Technology, Trondheim, Norway

<sup>3</sup>Delft University of Technology, Delft, The Netherlands

<sup>4</sup>Zhejiang University, Hangzhou, China

<sup>5</sup>Sapienza University of Rome, Rome, Italy

<sup>6</sup>Netherlands Organisation for Applied Scientific Research (TNO), Delft, The Netherlands

<sup>7</sup>Ghent University, Ghent, Belgium

## Correspondence

Morten Engen, Multiconsult Norge AS, Oslo, Norway.

Email: morten.engen@multiconsult.no

## Abstract

When non-linear finite element analyses are used in design of new or assessment of existing concrete structures, one should account for the modelling uncertainty before conclusions are drawn based on the results. The present article describes the basis for how this topic is treated in the draft of *fib* Model Code 2020. There are two components of the modelling uncertainty: (i) within-model, and (ii) between-model. The within-model uncertainty was estimated from a range of series of benchmark analyses gathered from the literature. Each series was assumed analyzed in a consistent manner, termed as the solution strategy. The main result for the within-model component, is a set of prior parameters for Bayesian updating. In an application setting, the prior parameters should be updated after validating the selected solution strategy with a suite of relevant benchmark analyses, before using the mean and coefficient of variation in the Global Factor Method or calculating the modelling uncertainty factor  $\gamma_{Rd}$  to be used in the Partial Factors Method. Finally, results from blind-prediction competitions were studied. With the present data, it cannot be concluded that a-priori knowledge of the experimental outcome reduces the uncertainty in the prediction. Hence, there is no need for compensating for this effect by a separate partial factor.

## KEYWORDS

design of concrete structures, Model Code 2020, modelling uncertainty, non-linear finite element analyses, safety format

## 1 | INTRODUCTION

In the final draft of the *fib* Model Code 2020, the chapter on non-linear finite element analyses (NLFEA) has been

reworked compared to the *fib* Model Code 2010.<sup>1</sup> A motivation for this revision was to build a strong link between the physical behavior that is being simulated, and the safety format that is applied. A key ingredient herein is the selected *solution strategy for NLFEA*. In the following, the term solution strategy is used to denote the method for performing the NLFEA. The solution strategy comprises all the choices related to (i) kinematic compatibility, for example, finite element types and sizes,

Discussion on this paper must be submitted within two months of the print publication. The discussion will then be published in print, along with the authors' closure, if any, approximately nine months after the print publication.

This is an open access article under the terms of the Creative Commons Attribution-NonCommercial-NoDerivs License, which permits use and distribution in any medium, provided the original work is properly cited, the use is non-commercial and no modifications or adaptations are made.

© 2021 The Authors. *Structural Concrete* published by John Wiley & Sons Ltd on behalf of International Federation for Structural Concrete.

(ii) equilibrium, for example, iterative solution method, and (iii) material models, for example, constitutive relations for concrete and reinforcement steel. The solution strategy also covers more problem-specific topics like discretization of the problem in time and space, idealization of the geometry and applied actions, and representation of boundary conditions, for example, constrained in single nodes with or without load-plates or contact relations between concrete and surrounding structures or foundations.

When a solution strategy is selected, the analyst should do a proper job in verifying and validating this. This means that the analyst should make sure that she *solves the equations right* and *solves the right equations*.<sup>2</sup> Checking the former involves *verification* of the solution strategy, where the analyst ensures that, for example, the sensitivity to finite element size and load step size is reasonably low, or that the incremental iterative method is adequate for capturing basic features of the intended material and structural behavior. Proper verification thus ensures that the uncertainty in the results from the simulations are related to idealization of the material, geometry, loads and boundary conditions. Checking of the latter involves *validation* of the solution strategy, where the analyst compares simulation outcomes with results from physical experiments, for example, reported in the literature, commonly denoted as benchmark analyses. Validation thus involves quantification of the modelling uncertainty. In the procedures outlined in this article, it is assumed that the analyst has performed proper verification of the solution strategy, such that the modelling uncertainty can be quantified by performing benchmark analyses.<sup>2-4</sup>

The selected solution strategy should be applied consistently during all the benchmark analyses, and furthermore during solution of the problem it is intended for. If not, the estimated modelling uncertainty cannot be guaranteed to cover the use. Ultimately, it is the responsibility of the analyst to ensure that the modelling uncertainty is properly accounted for before making decisions based on NLFEA results. One should never rely on software producers to take this responsibility, nor is it anticipated that any would do so.

This article presents the theoretical background for the modelling uncertainty for NLFEA of concrete structures the way this is treated in the present draft for *fib* Model Code 2020. Based on a systematic literature review, a set of statistical parameters for the modelling uncertainty are estimated, resulting in a set of prior parameters that could be the basis for Bayesian updating.

## 2 | QUANTIFICATION OF THE MODELLING UNCERTAINTY

### 2.1 | Components of the estimated modelling uncertainty

According to Engen<sup>5</sup> the following three limiting cases can be encountered in the literature where NLFEA predictions are compared to experimental outcomes:

1. One experimental outcome is compared to NLFEA predictions using different solution strategies, denoted as *The blind prediction competition*.
2. The outcomes of a number of nominally equal experiments are compared to one NLFEA prediction of the experiment using one solution strategy, denoted as *The scaled physical variability*.
3. One experimental outcome from each of a range of different experiments are compared to corresponding NLFEA predictions using one solution strategy, denoted as *Benchmarking of a solution strategy*.

Assuming that the modelling uncertainty generally takes the form of the ratio between the experimental outcome and the NLFEA prediction, that is,  $\theta = R_{\text{exp}}/R_{\text{NLFEA}}$ , the three limiting cases will have the following estimators

$$\theta_{1,k} = \frac{R_{\text{exp}}}{R_{\text{NLFEA},k}}, \theta_{2,j} = \frac{R_{\text{exp},j}}{R_{\text{NLFEA}}} \text{ and } \theta_{3,i} = \left( \frac{R_{\text{exp}}}{R_{\text{NLFEA}}} \right)_i. \quad (1)$$

By inspection of Equation (1) it is evident that  $\theta_1$  represents the uncertainty of the prediction if the solution strategy was selected randomly, that is, the *between-model uncertainty*,  $\theta_2$  represents the variability of the experimental outcome scaled with the model outcome, and  $\theta_3$  represents the uncertainty of the model outcome with one selected solution strategy, that is, the *within-model uncertainty*. The estimators in Equation (1) can be further generalized as

$$\theta_{ijk} = \left( \frac{R_{\text{exp},j}}{R_{\text{NLFEA},k}} \right)_i, \quad (2)$$

where the subscripts refer to experimental setup  $i$ , outcome  $j$  from experimental setup  $i$  and the NLFEA prediction of the experimental setup  $i$  using solution strategy  $k$ . Note that the term experimental setup refers to a specimen with given nominal geometry, reinforcement, material properties etc. and given support and loading conditions. The generalized estimator is shown

graphically in Figure 1 and systematically decomposed in Table 1.

Note that in the literature, usually only one experimental outcome is reported for each experimental setup, such that in Table 1,  $m_i = m = 1$ , and the generalized estimator in Equation (2) takes the form in Equation (3). There are, however, examples of experimental campaigns being repeated by independent researchers.

$$\theta_{ik} = \left( \frac{R_{\text{exp}}}{R_{\text{NLFEA},k}} \right)_i \quad (3)$$

When Equation (3) is used, the contributions to the estimate from within- and between-model uncertainty can be quantified by following a hierarchical approach as suggested by.<sup>6</sup>

Since the physical uncertainty of the experimental outcomes is usually not explicitly accounted for in the analyses, the estimate using Equation (3) implicitly includes this contribution. This contribution can only be eliminated if complete knowledge about the physical uncertainty of the experiments is obtained. In practice, this is hardly possible, however the user should be aware of it. If the physical uncertainty of the experiments can be represented by a single coefficient of variation,  $V_{\text{exp}}$ , and it can be assumed that the modelling uncertainty and the physical uncertainty are independent random variables, a simplified pure modelling uncertainty could

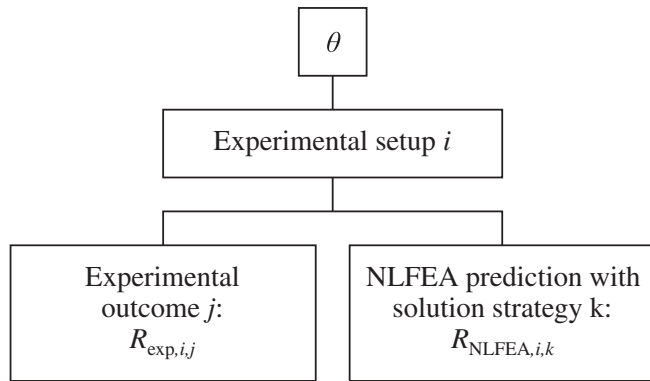


FIGURE 1 Graphical interpretation of the general estimator for the modelling uncertainty  $\theta$  in Equation (2)

	Experimental setup	Experimental outcome	NLFEA prediction
$\theta_{1,k}$	$i = I$	$j = J$	$k = [1, p_i]$
$\theta_{2,j}$	$i = I$	$j = [1, m_i]$	$k = K$
$\theta_{3,i}$	$i = [1, n]$	$j = J$	$k = K$

Note:  $p_i$  is the number of NLFEA predictions of experimental setup  $i$ ,  $m_i$  is the number of outcomes from experimental setup  $i$  and  $n$  is the number of experimental setups.

be estimated by subtraction, that is, following Equation (4).<sup>7,8</sup>

$$V_{\theta, \text{pure}} = \sqrt{V_{\theta}^2 - V_{\text{exp}}^2} \quad (4)$$

Assuming that the coefficient of variation obtained from Equation (3) is in the order of  $V_{\theta} \approx 0.1 - 0.15$  and that the physical uncertainties are in the order of  $V_{\text{exp}} \approx 0.05$ ,<sup>8,9</sup> the contribution from  $V_{\text{exp}}$  can be neglected. In the following, Equation (3) will be used as the basis for quantifying the modelling uncertainty.

## 2.2 | Method for quantifying the modelling uncertainty

It is assumed that the modelling uncertainty can be represented by a log-normally distributed random variable, that is, that  $y = \ln \theta$  is normally distributed. From a sample of  $n_k$  observations of the modelling uncertainty, the sample mean and variance can be calculated from

$$\bar{y}_k = \frac{1}{n_k} \sum_{i=1}^{n_k} y_i \quad (5)$$

and

$$s_k^2 = \frac{1}{n_k - 1} \sum_{i=1}^{n_k} (y_i - \bar{y}_k)^2. \quad (6)$$

Note that the subscript  $k$  indicates that the sample mean and variance belongs to solution strategy  $k$  out of the  $p$  available solution strategies. It can be shown that  $y$  can be represented by a  $t$ -distributed random variable with expected value and variance given in Equations (7) and (8), where  $\nu_k = n_k - 1$  are the degrees of freedom. See for example<sup>6</sup> for derivations. The mean and coefficient of variation of  $\theta$  can be estimated from Equations (9) and (10), where the errors of approximation in Equations (7) and (8) are  $<2\%$  for  $V_{\theta_k} < 0.2$ .<sup>6</sup>

TABLE 1 Systematic decomposition of the general estimator for the modelling uncertainty in Equation (2).

$$\mu_{y_k} = E[y_k] = \bar{y}_k \tag{7}$$

$$\sigma_{y_k}^2 = \text{VAR}[y_k] = \frac{\nu_k(\nu_k + 2)}{(\nu_k - 2)(\nu_k + 1)} s_k^2 \tag{8}$$

$$\mu_{\theta_k} = E[\theta_k] \approx \exp \bar{y}_k \tag{9}$$

$$V_{\theta_k} \approx \sqrt{\text{VAR}[y_k]} = s_k \sqrt{\frac{\nu_k(\nu_k + 2)}{(\nu_k - 2)(\nu_k + 1)}} \tag{10}$$

The effect of the degrees of freedom, that is, the number of observations or the decreasing statistical uncertainty, on the ratio between the calculated standard deviation  $\sigma_y$  and the sample standard deviation  $s_y$  is shown in Figure 2. Since the statistical uncertainty is significant if the estimate is based on a low number of observations, the resulting coefficient of variation should always be estimated using Equation (10).

If results from benchmark analyses of  $p$  different solution strategies are collected, and the mean and coefficient of variation of the complete sample is calculated according to Equations (7) and (8), it is evident that the estimate includes a component of the between-model uncertainty. An alternative method which can be used to estimate a pure within-model uncertainty is the method of maximum likelihood estimators (MLE) as derived, for example, [6].

The MLE for the sample variance, the degree of knowledge about the sample variance, the sample mean, and the degree of knowledge about the sample mean, are shown in Equations (11–14), with parameters in Equation (15). According to Engen<sup>6</sup>, the error term in Equation (12) is due to truncation after second order terms in the derivation. Herein, this error term is compensated for by solving iteratively for  $\nu_{\text{MLE}}$  as suggested in [6]. As

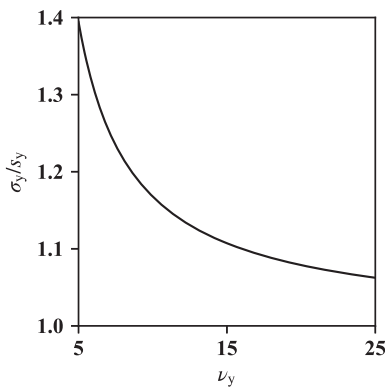


FIGURE 2 The ratio of the standard deviation  $\sigma_y$  to the sample standard deviation  $s_y$  as function of the degrees of freedom  $\nu_y$

demonstrated by Engen<sup>6</sup> the MLE can be used as prior parameters that can be updated using a Bayesian updating technique.

$$s_{\text{MLE}}^2 = \frac{1}{A} \tag{11}$$

$$\nu_{\text{MLE}} = \frac{1}{\ln A - B - e(\nu_{\text{MLE}}^2)} \approx \frac{1}{\ln A - B} \tag{12}$$

$$\bar{y}_{\text{MLE}} = \frac{C}{A} \tag{13}$$

$$n_{\text{MLE}} = \frac{1}{D - C^2/A} \tag{14}$$

$$A = \frac{1}{p} \sum_{k=1}^p \frac{1}{s_k^2}, \quad B = \frac{1}{p} \sum_{k=1}^p \ln \frac{1}{s_k^2}, \quad C = \frac{1}{p} \sum_{k=1}^p \frac{\bar{y}_k}{s_k^2}, \quad D = \frac{1}{p} \sum_{k=1}^p \frac{\bar{y}_k^2}{s_k^2} \tag{15}$$

If a solution strategy is validated by performing a series of benchmark analyses, the values for  $\mu_\theta$  and  $V_\theta$  of this specific solution strategy should be calculated by considering Bayesian updating of prior parameters with the sample mean and variance from the series of benchmark analyses. The basic equations for Bayesian updating are given in Equations (16–19), and derivations can be found in<sup>6,10</sup>. In Equations (16–19)  $s'$ ,  $\nu'$ ,  $\bar{y}'$  and  $n'$  are the prior parameters for the statistical parameters,  $s$ ,  $\nu$ ,  $\bar{y}$  and  $n$  are the results from the series of benchmark analyses and  $s''$ ,  $\nu''$ ,  $\bar{y}''$  and  $n''$  are the updated statistical parameter that should be input to Equations (9) and (10).

$$s''^2 = \frac{1}{\nu''} (\nu s^2 + \nu' s'^2 + n \bar{y}^2 + n' \bar{y}'^2 - n'' \bar{y}''^2) \tag{16}$$

$$\nu'' = \nu' + \nu + 1 \tag{17}$$

$$\bar{y}'' = \frac{1}{n''} (n \bar{y} + n' \bar{y}') \tag{18}$$

$$n'' = n' + n \tag{19}$$

When proper values for  $\mu_\theta$  and  $V_\theta$  are obtained, a modelling uncertainty factor  $\gamma_{\text{RD}}$  can be calculated according to Equation (20). In Equation (20),  $\alpha_{\text{R}}$  is the sensitivity factor for the resistance modelling uncertainty, and  $\beta$  is the target reliability index.

$$\gamma_{\text{RD}} = \frac{1}{\mu_\theta} \exp \alpha_{\text{R}} \beta V_\theta = \frac{1}{\mu_\theta} \exp \alpha_{\text{R}} \beta s \sqrt{\frac{\nu}{\nu - 2} \frac{\nu + 2}{\nu + 1}} \tag{20}$$

The modelling uncertainty factor can alternatively be calculated from the  $t$ -distribution according to Equation (21) where  $\Phi^{-1}(\alpha_R\beta)$  is the probability corresponding to the fractile  $z = \alpha_R\beta$  of the standard normal distribution.

$$\begin{aligned} \gamma_{Rd} &= \frac{1}{\exp\left(\bar{y} - t_{\Phi^{-1}(\alpha_R\beta), \nu} s \sqrt{\frac{\nu+2}{\nu+1}}\right)} \\ &= \frac{1}{\mu_\theta} \exp\left(t_{\Phi^{-1}(\alpha_R\beta), \nu} s \sqrt{\frac{\nu+2}{\nu+1}}\right) \end{aligned} \quad (21)$$

The modelling uncertainty factor expressed as in Equation (20) converges to Equation (21) as shown in Figure 3a, and is conservative for lower values of  $\nu$ . The conservatism lies in the assumption of an unknown variance when deriving Equation (8), resulting in the equivalent fractile shown in Figure 3b. In the following, the modelling uncertainty factor will be calculated using Equation (20). Figure 4 demonstrates the effect of the degrees of freedom on the calculated modelling uncertainty factor for different sample standard deviations.

### 3 | RESULTS

#### 3.1 | General

In this section, the modelling uncertainty will be quantified based on a systematic literature review and the methodology outlined above. Based on these results, prior parameters for Bayesian updating and a given value for  $\gamma_{Rd}$  will be estimated. Note that the prior parameters should represent only the within-model component of the uncertainty, since these are used together with results using one specific solution strategy, and the resulting statistical parameters should be relevant for that specific solution strategy. On the other hand, the given value of

$\gamma_{Rd}$  should in addition include the between-model component, since this should be used in exceptional cases where the solution strategy is only selected from a range of available solution strategies, verified, and furthermore applied without thorough validation.

#### 3.2 | Review of results from benchmarking of solution strategies

Figure 5 shows schematically how the results from benchmark analyses using a set of solution strategies can be compiled in a two-dimensional array. Each solution strategy is benchmarked with all or a subset of the experiments. Note that the array is usually sparse, since not all solution strategies are benchmarked with the same experiments. The within-model component of the modelling uncertainty can be estimated by calculating the sample means and standard deviations vertically in the array, that is, per solution

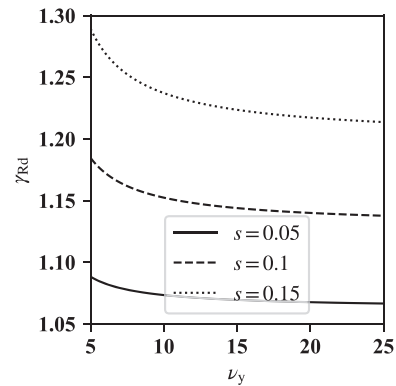


FIGURE 4 The modelling uncertainty factor  $\gamma_{Rd}$  as function of the degrees of freedom  $\nu_y$  for different values of the sample standard deviation  $s$  assuming a bias  $\bar{y} = 0$ , and  $\alpha_R = 0.4 \cdot 0.8$  and  $\beta = 3.8$  for 50 years

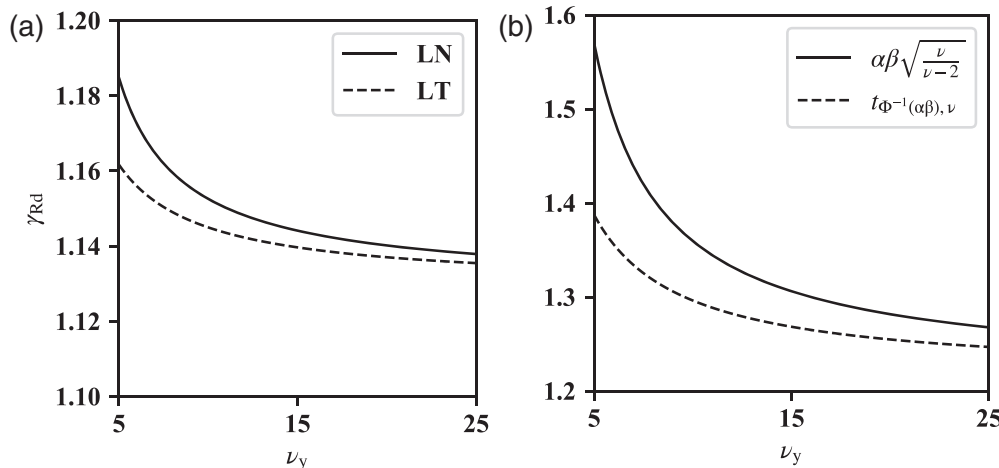


FIGURE 3 (a) Comparison of Equation (20) (LN) and (21) (LT) assuming  $s = 0.10$  and  $\bar{y} = 0.0$ , (b) the equivalent fractiles in the former

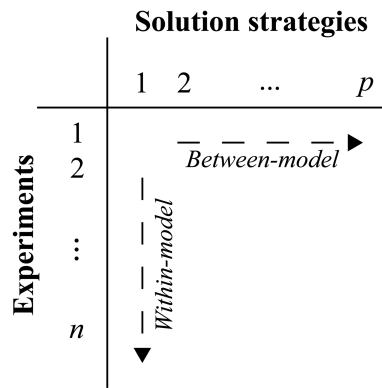


FIGURE 5 Schematic representation of calculating within-model and between-model uncertainty from benchmark analysis results using a series of  $p$  solution strategies, each solving all or a subset of the  $n$  experiments. The arrows indicate the direction for calculating sample statistics

strategy. The between-model component, on the other hand, is estimated horizontally, that is, per experiment.

Table 2 shows an overview of results from benchmarking of 27 different solution strategies found in the literature. All results are from trusted sources, where it is reasonable to assume that the solution strategy was applied consistently in all analyses. The results in Table 2 represent  $\theta_3$ , as defined in Equation (1), calculating vertically as demonstrated in Figure 5. The bias in Table 2 is on average close to 1.0, and the modelling uncertainty can be safely assumed to be unbiased. The coefficient of variation of the complete sample is relatively low and almost converged towards the sample standard deviation due to the large number of observations, ref. Figure 2.

Table 3 shows the results from the MLE based on the results in Table 2. Since the degrees of belief in the mean and the standard deviation, that is,  $n_{MLE}$  and  $\nu_{MLE}$ , in

TABLE 2 Results from benchmarking of different solution strategies.

References	$\bar{y}_k$	$s_{y,k}^2$	$n_k$	$\mu_{\theta_k}$	$V_{\theta_k}$
Engen et al. <sup>2</sup>	0.092	0.011	38	1.103	0.110
Engen et al. <sup>16</sup>	0.117	0.036	10	1.154	0.229
Kotsovos & Pavlovic, 2D <sup>17</sup>	0.000	0.028	24	1.016	0.179
Kotsovos & Pavlovic, 3D <sup>17</sup>	0.091	0.009	23	1.100	0.099
Belletti et al. <sup>18</sup>	0.120	0.033	13	1.152	0.210
Bertagnoli et al., A1 <sup>11</sup>	0.017	0.009	16	1.023	0.105
Bertagnoli et al., A2 <sup>11</sup>	0.026	0.007	16	1.030	0.094
Bertagnoli et al., B1 <sup>11</sup>	0.120	0.006	16	1.132	0.089
Bertagnoli et al., B2 <sup>11</sup>	0.182	0.006	16	1.204	0.083
Bertagnoli et al., C1 <sup>11</sup>	-0.058	0.011	16	0.950	0.116
Bertagnoli et al., C2 <sup>11</sup>	0.057	0.010	16	1.065	0.113
Belletti et al. <sup>19</sup>	0.055	0.004	11	1.060	0.076
Kadlec & Cervenka <sup>20</sup>	-0.041	0.007	10	0.965	0.100
Muttoni et al. <sup>21</sup>	0.031	0.009	315	1.036	0.094
Selby & Vecchio <sup>22</sup>	0.018	0.021	22	1.030	0.156
Castaldo et al., M1 <sup>12</sup>	-0.005	0.011	16	1.002	0.118
Castaldo et al., M2 <sup>12</sup>	-0.008	0.013	16	1.000	0.127
Castaldo et al., M3 <sup>12</sup>	-0.014	0.010	16	0.992	0.111
Castaldo et al., M4 <sup>12</sup>	-0.107	0.008	16	0.903	0.100
Castaldo et al., M5 <sup>12</sup>	-0.098	0.009	16	0.912	0.107
Castaldo et al., M6 <sup>12</sup>	-0.170	0.007	16	0.848	0.096
Castaldo et al., M7 <sup>12</sup>	0.069	0.013	16	1.080	0.127
Castaldo et al., M8 <sup>12</sup>	0.043	0.011	16	1.051	0.115
Castaldo et al., M9 <sup>12</sup>	-0.044	0.015	16	0.966	0.136
Cervenka et al. <sup>23</sup>	0.005	0.006	33	1.009	0.084
Pimentel, F <sup>24</sup>	0.032	0.002	15	1.034	0.053
Pimentel, R <sup>24</sup>	0.054	0.009	15	1.061	0.105
<b>All</b>	<b>0.026</b>	<b>0.013</b>	<b>769</b>	<b>1.034</b>	<b>0.117</b>



Table 3 are only moderate, this indicates that the modelling uncertainty of the different solution strategies in Table 2 do not all come from the same population. The results at the lower row of Table 2 should therefore not be used as basis for a general modelling uncertainty factor. The parameters in Table 3, however should be interpreted as the *typical* statistical parameters of the modelling uncertainty, neglecting the contribution from between-model uncertainty. The results in Table 3 correspond to  $\mu_{\theta,w} = 1.020$ ,  $V_{\theta,w} = 0.13$  and  $\gamma_{Rd,w} = 1.15$  assuming  $\alpha_R = 0.4 \cdot 0.8$  and  $\beta = 3.8$  for 50 years, where the subscript  $w$  indicates that only the within-component is included.

There are two subsets of Table 2 that are particularly interesting<sup>11,12</sup> since these contain 16 experiments, simulated with 15 different solution strategies. This subset can thus be represented as a full array as in Figure 5, and can give more insight in the between-model uncertainty. By applying the method of MLE on each series of numerical simulations of each experiment, the results in Table 4 are obtained. These results thus represent  $\theta_1$  as defined in Equation (1). The results in Table 4 correspond to  $\mu_{\theta,b} = 1.0$ ,  $V_{\theta,b} = 0.14$  and  $\gamma_{Rd,b} = 1.18$  assuming  $\alpha = 0.4 \cdot 0.8$  and  $\beta = 3.8$  for 50 years, where the subscript  $b$  indicates that only the between-component is included.

A given value for the modelling uncertainty factor can be obtained by multiplying the factors for the within- and between-components, that is,  $\gamma_{Rd} = \gamma_{Rd,w} \gamma_{Rd,b} \approx 1.35$ , assuming that these are independent. Note that this value is estimated based on results from static NLFEA predictions of failure loads. Other contributions are also reporting predictions of the deformations and capacity of cyclically loaded structural elements, for example [13,14], and the given value for  $\gamma_{Rd}$  is also representative for these results. The components of  $\gamma_{Rd}$  are summarized in Table 5.

### 3.3 | Review of results from blind-prediction competitions

Table 6 shows an overview of results from blind-prediction competitions found in the literature and Table 7 shows

**TABLE 3** Results from MLE based on the results in Table 2, where  $s_{MLE}$ ,  $\nu_{MLE}$ ,  $\bar{y}_{MLE}$ , and  $n_{MLE}$  are the prior parameters for the modelling uncertainty.

A	B	C	D
118.532	4.606	2.698	0.756
$s_{MLE}$	$\nu_{MLE}$	$\bar{y}_{MLE}$	$n_{MLE}$
0.092(0.10)	6.224(6.20)	0.023(0.02)	1.44(1.40)

Note: The values in parentheses are rounded values suitable for codification.

results from MLE based on Table 6. Note that the results in Table 7 are not intended to be used as prior parameters. The results in Table 6 can be interpreted in a similar manner as those in Table 4, representing the between-model component and  $\theta_1$  as defined in Equation (1). The essential difference between the results in Tables 4 and 6 is that the latter is based on analyses performed without knowing the experimental result on beforehand, a situation closely related to engineering practice.

Based on simple hypothesis testing, that is, *t-test* for the mean and *F-test* for the variance, the null-hypotheses that the variances and means are equal cannot be rejected, see the results in Table 8. Note that the *P-value* is the probability of observing the results in Tables 4 and 6, given that the null-hypothesis is true. The null-hypotheses can alternatively be formulated as *knowing the experimental outcome a priori does not improve the estimate*. Since this cannot be rejected, the present results indicate that there is not sufficient evidence for introducing additional factors to account for any bias due to knowing the experimental outcome before running the benchmark analysis.

## 4 | APPLICATION EXAMPLE

### 4.1 | General

This section gives an example on how to utilize the results from the proceeding sections. The statistical parameters of the modelling uncertainty, and furthermore the modelling uncertainty factor  $\gamma_{Rd}$ , should be calculated by the following standard procedure:

1. Collect a set of experiments reported in the literature that are relevant for the problem which is to be solved.

**TABLE 4** Results from MLE based on the sample statistics per experiment in.<sup>11,12</sup>

A	B	C	D
72.460	4.178	-0.032	0.044
$s_{MLE}$	$\nu_{MLE}$	$\bar{y}_{MLE}$	$n_{MLE}$
0.117	9.830	0.000	22.519

**TABLE 5** Components of the given value of  $\gamma_{Rd}$  as described above.

<b>Within-model</b>	$\gamma_{Rd,w} = 1.15$
<b>Between-model</b>	$\gamma_{Rd,b} = 1.18$
<b>Total</b>	$\gamma_{Rd} = \gamma_{Rd,w} \gamma_{Rd,b} \approx 1.35$

**TABLE 6** Results from blind-prediction competitions found in the literature.

References	$\bar{y}$	$s_{y,k}^2$	$n$	$\mu_{\theta_k}$	$V_{\theta_k}$
Collins et al., Panel A <sup>25</sup>	-0.124	0.032	27	0.899	0.192
Collins et al., Panel B <sup>25</sup>	0.113	0.156	27	1.223	0.437
Collins et al., Panel C <sup>25</sup>	-0.011	0.050	27	1.017	0.240
Collins et al., Panel D <sup>25</sup>	-0.237	0.170	27	0.869	0.459
van Mier & Ulfkjær, Small <sup>26</sup>	0.078	0.012	8	1.092	0.140
van Mier & Ulfkjær, Large <sup>26</sup>	0.065	0.014	8	1.079	0.147
Jaeger & Marti, A1 <sup>27</sup>	-0.165	0.079	8	0.902	0.363
Jaeger & Marti, A2 <sup>27</sup>	-0.093	0.011	8	0.920	0.134
Jaeger & Marti, B1 <sup>27</sup>	0.076	0.073	8	1.143	0.348
Jaeger & Marti, B2 <sup>27</sup>	0.054	0.004	8	1.059	0.083
Jaeger & Marti, C1 <sup>27</sup>	-0.241	0.103	8	0.852	0.420
Jaeger & Marti, C2 <sup>27</sup>	-0.101	0.011	8	0.912	0.132
Jaeger & Marti, D1 <sup>27</sup>	0.029	0.073	8	1.090	0.348
Jaeger & Marti, D2 <sup>27</sup>	0.121	0.001	8	1.130	0.046
Collins et al., first failure <sup>28</sup>	-0.363	0.297	66	0.813	0.604
Collins et al., second failure <sup>28</sup>	0.108	0.109	43	1.181	0.352
Strauss et al. <sup>29</sup>	-0.126	0.004	8	0.884	0.075

**TABLE 7** Results from MLE based on the results in Table 6.

A	B	C	D
100.362	3.467	3.035	1.226
$s_{MLE}$	$\nu_{MLE}$	$\bar{y}_{MLE}$	$n_{MLE}$
0.100	1.375	0.030	0.88

2. Select the solution strategy and apply this consistently in numerical simulations of each of the collected experiments.
3. Based on the results from each  $i$  benchmark analysis, calculate the ratio  $\theta_i = \left(\frac{R_{exp}}{R_{NLFEA}}\right)_i$  and  $y_i = \ln \theta_i$ , and calculate the sample mean and standard deviation using Equations (5) and (6). Note that  $n_k$  in the latter equations refer to the number of collected experiments that are used in the validation.
4. Using the sample statistics calculated in pt. 3, the prior parameters in Table 3 should be updated according to Equations (16–19).
5. The mean, coefficient of variation and modelling uncertainty factor should be calculated using Equations (9), (10), and (20) and the posterior parameters from pt. 4.

### 4.2 | Update prior parameters with results from benchmark analyses

In Reference [15], a series of experiments on structural walls are analyzed with NLFEA. Table 9 shows how the

**TABLE 8** Results from hypothesis testing based on the results in Tables 4 and 7.

Mean	
$H_0: \mu_1 - \mu_2 = 0$	
$H_1: \mu_1 - \mu_2 \neq 0$	
$t = 0.372$	Do not reject
$t_{max} = 2.196$	
$P = 0.359 > 0.05$	
Variance	
$H_0: \sigma_1 = \sigma_2$	
$H_1: \sigma_1 \neq \sigma_2$	
$F_{min} = 0.160$	Do not reject
$F_{max} = 6.231$	
$F = 1.385$	
$P = 0.460 > 0.05$	

Note: Note that the bounds for the tests are found by assuming a 5% level of significance.

results from the study in Reference [15] can be used to update the prior parameters for the modelling uncertainty. The numbers under *Prior* are taken from Table 3. The results under *Additional results* are derived from the results in Reference [15] using Equations (5) and (6). The bias indicates that the results are on average conservative. In Reference [15], this is explained to be due to a conservative representation of the compressive behavior in experiments where a significant degree of confinement

**TABLE 9** Results from updating the prior parameters for the modelling uncertainty with the additional results from.<sup>15</sup>

	Prior	Additional results <sup>15</sup>	Posterior
$s$	0.10	0.064	0.098
$\nu$	6.20	5	12.20
$\bar{y}$	0.02	0.197	0.164
$n$	1.40	6	7.40
$\mu_\theta$	–	1.22	1.19
$V_\theta$	–	0.09	0.11
$\gamma_{Rd}$	–	0.91	0.97

can be present. The mean, coefficient of variation and modelling uncertainty factor are calculated using Equations (9), (10), and (20). Due to the high bias, the resulting  $\gamma_{Rd}$  is less than unity if only the results from Reference [15] are taken into account. The numbers under *Posterior* are results from updating the prior parameters with the additional results using Equations (16–19). This gives a larger coefficient of variation and a slightly lower mean, and a modelling uncertainty factor closer to unity.

These results illustrate two important aspects:

1. By providing prior parameters for updating, the analyst is encouraged to run benchmark analyses and calculate the statistical parameters and a resulting  $\gamma_{Rd}$  which is representative for the selected solution strategy and lower than the given value.
2. The prior parameters ensure that the analyst can obtain a relevant  $\gamma_{Rd}$ , but at the same time take into account possible uncertainties that are not uncovered in the benchmark analyses.

## 5 | DISCUSSION AND CONCLUSION

The main challenge of applying NLFEA in design of new or assessment of existing concrete structures, is that the result is not known on beforehand. The present results indicate, however, that the effort that is put into investigating the failure mode in the analysis results, as illustrated in the study of the blind-prediction competitions, balances this. The results in the present study do not support including a separate factor to account for this challenge.

The validation of the solution strategy should be based on several benchmark analyses relevant for the problem at hand. No lower limit is put on the number of benchmark analyses, but at least 2-3 should be included

for the results of Equation (6) to be meaningful. If the prior parameters derived herein are used, the value of the degrees of freedom is sufficiently high to guarantee stability of the  $t$ -distribution. Note, however, that the analyst has a strong incentive to increase the number of benchmark analyses, since this has direct influence on the coefficient of variation expressed as Equation (10). This is considered elegant, compared to, for example, introducing a separate partial factor to cover the statistical uncertainty.

The prior parameters represent the within-model uncertainty. Judging based on the degrees of belief, the mean is rather vague, which is useful if the selected solution strategy is strongly biased. On the other hand, the standard deviation is relatively strong ensuring that the posterior coefficient of variation is steered towards the typical value if a small sample of benchmark experiments is selected.

The analyst can never put the responsibility on other parties to validate the selected solution strategy. At the same time, it is not always possible to perform a thorough validation of the selected solution strategy, for example, due to time constraints or lack of relevant experiment results. In such cases, the solution strategy could be interpreted as being selected randomly from the population of solution strategies, without knowledge of its actual behavior. This is respected by including the between-model component in the given value for  $\gamma_{Rd}$ . The solution strategy should however always be properly verified. Eventually, the value  $\gamma_{Rd} = 1.35$  is a strong incentive for investing in benchmarking, building a stronger link between the physical behavior that is being simulated, and the safety format that is applied.

## ACKNOWLEDGMENTS

The study presented herein is a result of the work carried out by the *Coordination and Drafting Group* of *fib* TG.10.1, AG8 *Non-linear Finite Element Modelling* in preparing the final draft for *fib* Model Code 2020. Preliminary results have been discussed on several occasions in *fib* TG3.1, and any feedback has been highly appreciated.

## DATA AVAILABILITY STATEMENT

The data that support the findings of this study are available from the corresponding author upon reasonable request.

## ORCID

Morten Engen  <https://orcid.org/0000-0002-9787-2010>

## REFERENCES

1. fib. *fib* Model Code for concrete structures. Vol 2013. Lausanne: Ernst & Sohn; 2010.

2. Engen M, Hendriks MAN, Köhler J, Øverli JA, Åldstedt E. Quantification of the modelling uncertainty of non-linear finite element analyses of large concrete structures. *Struct Saf.* 2017; 64(1):1–8.
3. Taerwe L. Model uncertainties in reliability formats for concrete structures. *CEB Bulletin 224*. Lausanne: Comité Euro-International du Béton; 1995. p. 5–7.
4. Sykora M, Krejsa J, Mlcoch J, Prieto M, Tanner P. Uncertainty in shear resistance models of reinforced concrete beams according to fib MC2010. *Struct Concr.* 2018;19:284–95.
5. M. Engen, 2017, Aspects of design of reinforced concrete structures using non-linear finite element analyses, Trondheim: Doctoral Thesis, NTNU.
6. Engen M, Hendriks MAN, Köhler J, Øverli JA, Åldstedt E, Mørtzell E, et al. Predictive strength of ready-mixed concrete: exemplified using data from the Norwegian market. *Struct Concr.* 2018;19:806–19.
7. Pinglot M, Duprat F, Lorrain M. An analysis of model uncertainties: ultimate limit state of buckling. *CEB Bulletin 224*. Lausanne: Comité Euro-International du Béton; 1995. p. 9–48.
8. Holický M, Retief JV, Sykora M. Assessment of model uncertainties for structural resistance. *Probabilistic Eng Mech.* 2016; 45:188–97.
9. Sykora M, Holický M, Prieto M, Tanner P. Uncertainties in resistance models for sound and corrosion-damaged RC structures according to EN 1992-1-1. *Mater Struct.* 2015;48:3415–30.
10. Gelman A, Carlin JB, Stern HB, Dunson DB, Vehtari A, Rubin DB. *Bayesian Data Analysis*. Boca Raton, Florida, USA: CRC Press; 2014.
11. Bertagnoli G, La Mazza D, Mancini G. Effect of concrete tensile strength in non linear analyses of 2D structures: a comparison between three commercial finite element software. 3rd International Conference on Advances in Civil. Rome: Structural and Construction Engineering - CSCE; 2015. p. 104–11.
12. Castaldo P, Gino D, Bertagnoli G, Mancini G. Partial safety factor for resistance model uncertainties in 2D non-linear finite element analysis of reinforced concrete structures. *Eng Struct.* 2018;176:746–62.
13. Gino D, Bertagnoli G, La Mazza D, Mancini G. A quantification of model uncertainties in NLFEA of R.C. shear walls subjected to repeated loading. *Ingegneria Sismica.* 2017;11(3): 79–91.
14. Castaldo P, Gino D, Bertagnoli G, Mancini G. Resistance model uncertainty in non-linear finite element analyses of cyclically loaded reinforced concrete systems. *Engineering Structures.* 2020;211:1–32.
15. Nilsen-Nygaard I. Structural safety assessment of reinforced concrete structures with nonlinear finite element analyses and the significance of the modelling uncertainty (M.Sc. Thesis). NTNU: Trondheim; 2015.
16. Engen M, Hendriks MAN, Øverli JA, Åldstedt E. Solution strategy for non-linear finite element analyses of large reinforced concrete structures. *Struct Concr.* 2015;16(3): 389–97.
17. Kotsovos MD, Pavlovic MN. *Structural concrete: finite-element analysis for limit-state design*. London: Thomas Telford; 1995.
18. Belletti B, Damoni C, Hendriks MAN, de Boer A. RTD: 1016-2: 2017: validation of the guidelines for nonlinear finite element analysis of concrete structures. Utrecht: Rijkswaterstaat Centre for Infrastructure; 2017.
19. Belletti B, Pimentel M, Scolari M, Walraven JC. Safety assessment of punching shear failure according to the level of approximation approach. *Structural Concrete.* 2015;16(3): 366–380.
20. Kadlec L, Cervenka V. Uncertainty of numerical models for punching resistance of RC slabs. *Concrete: Innovation and Design, fib Symposium*. Copenhagen; Fédération internationale du béton; 2015.
21. Muttoni A, Fernández Ruiz M, Niketic F, Backes M-R. Assessment of existing structures based on elastic-plastic stress fields: modelling of critical details and investigations of the in-plane shear transverse bending interaction. Vol 680. Lausanne: Structural Concrete Laboratory of EPFL; 2016.
22. Selby RG, Vecchio FJ. Three-dimensional constitutive relations for reinforced concrete, publication no. 93-02. Toronto: University of Toronto, Department of Civil Engineering; 1993.
23. Cervenka V, Cervenka J, Kadlec L. Model uncertainties in numerical simulations of reinforced concrete structures. *Struct Concr.* 2018;19(6):2004–2016.
24. Pimentel MJDS. Numerical modelling for safety examination of existing concrete bridges. Porto: Faculty of Engineering of the University of Porto; 2011.
25. Collins MP, Vecchio FJ, Mehlhorn G. An international competition to predict the response of reinforced concrete panels. *Canad J Civ Eng.* 1985;12:624–44.
26. van Mier JGM, Ulfkjær JP. Round-Robin analysis of over-reinforced concrete beams - comparison of results. *Mater Struct.* 2000;33:381–90.
27. Jaeger T, Marti P. Reinforced concrete slab shear prediction competition: entries and discussion. *ACI Struct J.* 2009;106(3):309–18.
28. Collins MP, Bentz EC, Quach PT, Proestos GT. The challenge of predicting the shear strength of very thick slabs. *Concr Int.* 2015;37(11):29–37.
29. Strauss A, Eschbacher T, Kendický P, Benko V. Tragkapazität schlanker Druckglieder. Teil 1: Bauteilversuche und Ringversuch der nichtlinearen numerischen Prognose des Systemverhaltens. *Beton- und Stahlbetonbau.* 2015;110(12): 845–56.

## AUTHOR BIOGRAPHIES



**Morten Engen**, Multiconsult AS, Department for Structural Analyses, Postboks 265 Skøyen, 0276 Oslo. Adjunct Associate Professor, Norwegian University of Science and Technology, NTNU, Department of Structural Engineering, Richard Birkelands vei 1A, 7491 Trondheim, Norway.



**Max A. N. Hendriks**, Professor, Delft University of Technology, Faculty of Civil Engineering and Geosciences, Steinweg 1, 2628 CNDelft, The Netherlands. Professor, Norwegian University of Science and Technology, NTNU, Department of Structural Engineering, Richard Birkelands vei 1A, 7491 Trondheim, Norway.



**Giorgio Monti**, Professor, Zhejiang University, College of Civil Engineering and Architecture, Yuhangtang Road, 866, 310058 Hangzhou, China. Professor, Sapienza University of Rome, Department of Structural Engineering and Geotechnics, Via A. Gramsci, 53, 00197 Rome, Italy.



**Diego L. Allaix**, Netherlands Organisation for Applied Scientific Research (TNO), Department of Structural Reliability, Stieltjesweg 1, 2628 CK Delft, The Netherlands. Associate Professor, Ghent University, Faculty of Engineering and Architecture, Department of Structural Engineering and Building Materials, Technologie park Zwijnaarde 60, 9052Z Zwijnaarde, Belgium.

**How to cite this article:** Engen M, Hendriks MAN, Monti G, Allaix DL. Treatment of modelling uncertainty of NLFEA in *fib* Model Code 2020. *Structural Concrete*. 2021;22:3202–12. <https://doi.org/10.1002/suco.202100420>